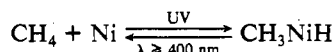


Figure 3. Photolysis study in an argon matrix ($\text{Ni}/\text{CH}_4/\text{Ar} \approx 0.7/1.8/100$): (A) before photolysis; (B) after 10-min photolysis with $380 \text{ nm} \geq \lambda \geq 280 \text{ nm}$; (C) after 10-min photolysis with $\lambda \geq 400 \text{ nm}$.

concentration study and molecular isotopic studies, respectively. Partial spectra of CH_3NiH , $^{13}\text{CH}_3\text{NiH}$, and CD_3NiD in methane and argon matrices are presented in Figures 1 and 2. In methane matrices the product absorptions are very weak and are split possibly due to matrix site effects.⁵ The measured frequencies and assignments of these weak absorptions as well as those obtained in argon matrices are presented in Table I.

The observed splittings of the Ni-H stretch and methyl deformation in a methane matrix indicate a significant matrix-molecule interaction and appreciable population of two matrix sites. This may be compared to the case in an argon matrix, where the molecule is produced in essentially one site. Significant interaction of CH_3NiH with the methane matrix is also indicated by the large positive shift of the methyl deformation mode. The size of this shift from an argon matrix to a methane matrix ($\sim 95 \text{ cm}^{-1}$) is large when compared to similar shifts for iron and manganese ($\sim -5 \text{ cm}^{-1}$) and is in the opposite direction. The magnitude of this shift suggests that methane acts as a weakly interacting ligand.

A photoreversible oxidative-addition/reductive-elimination reaction⁶ was also observed in this study as depicted in Figure 3. Thus, in an argon matrix (Figure 3A) the insertion product CH_3NiH was formed after UV irradiation (Figure 3B) but $\lambda \geq 400 \text{ nm}$ photolysis caused the complete disappearance of this species (Figure 3C):



The observation of photoinsertion of atomic nickel into methane shows then that all of the metal atoms from manganese to zinc undergo photoinsertion into methane. The lack of photoinsertion for the first half of the 3d-transition-metal series¹ suggests that the photoinsertion product for these metals is not physically stable and reverts readily to methane and the respective metal atom.

Acknowledgment. The financial support of the National Science Foundation, the 3M Co., and The Robert A. Welch Foundation are greatly appreciated.

Registry No. CH_4 , 74-82-8; Ni, 7440-02-0; CH_3NiH , 86392-32-7; $^{13}\text{CH}_3\text{NiH}$, 110638-26-1; CD_3NiD , 110638-27-2.

Supplementary Material Available: Figure showing the FTIR spectrum from 500 to 3500 cm^{-1} of a Ni/CH_4 reaction and photochemistry in an Ar matrix at 12 K (1 page). Ordering information is given on any current masthead page.

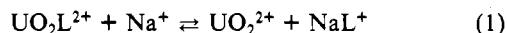
Contribution from UA 405 au CNRS, Ecole Européenne des Hautes Etudes des Industries Chimiques de Strasbourg, 1, rue Blaise Pascal, 67000 Strasbourg, France

Metal-Exchange Reactions between the Uranyl-18-Crown-6 Complex and Na^+ Ion in Propylene Carbonate

Pierre Fux, Janine Lagrange, and Philippe Lagrange*

Received March 10, 1987

In this paper we report a new aspect of crown ether kinetics: a metal-exchange reaction between the uranyl ion and sodium ion in the 18-crown-6 ether (L) complex



in propylene carbonate (PC) medium ($[(\text{C}_2\text{H}_5)_4\text{NClO}_4] = 0.1 \text{ M}$).

Actually, kinetic studies on crown ether complexes have been quite sparse. The main results concern principally alkali-metal- and alkaline-earth-cation complexation (complex formation or decomplexation). These reactions have been the subject of great interest because of their suitability as models for biochemical processes. Only very few kinetic studies on crown ethers have focused on other metals or polyatomic units. For example Eyring et al.^{1,2} have determined the complexation rate constant of Ti^+ , Ag^+ , and NH_4^+ cations with the 18-crown-6 ligand. The rates of all these complexation reactions are very fast. In particular, the rate of complexation of the Na^+ ion with 18-crown-6^{1,3-7} in water or in various solvents is almost diffusion controlled. Our recent study⁸ on the complexation of the 18-crown-6 ether with the uranyl ion has shown a formation rate constant several orders of magnitude lower than those normally encountered for alkali-metal or alkaline-earth cations complexed by the same ligand. Then kinetic measurements could be carried out by stopped-flow spectrophotometry.

It appears in all these kinetic studies that the short-range interactions are very important. In particular, the macrocycle ligand and the solvent molecules are competitors for the first coordination sphere of the cations.

Experimental Section

All chemicals were analytical reagent grade. The crown ether 18-crown-6 (1,4,7,10,13,16-hexaoxacyclooctane) and sodium perchlorate were purchased from Merck. Tetraethylammonium perchlorate and propylene carbonate were obtained from Fluka, and uranium perchlorate was purchased from Ventron GmbH. The perchlorate salts were dried under vacuum. PC was purified according to the method of Gosse,⁹ all the solutions in PC contained after purification less than 100 ppm of H_2O . The concentration of the uranyl ion was determined by polarography.¹⁰ The ionic strength was maintained constant at 0.1 M by addition of $(\text{C}_2\text{H}_5)_4\text{NClO}_4$.

The rates of the metal-exchange reaction were determined by means of a spectrophotometric technique. The stopped-flow spectrophotometer, a Durrum Gibson type equipped with a Datalab DL 905 transient recorder, was interfaced to an Apple II microcomputer. This system and the computer programs used have been previously described.¹¹ Reaction rates were followed at 290 nm and at $25.0 \pm 0.1^\circ \text{C}$. At this wavelength the greatest change in absorption between reagents and products was found. Kinetic runs were performed by mixing a UO_2L^{2+} solution ($[\text{UO}_2\text{L}^{2+}]_0 = 1.375 \times 10^{-4} \text{ M}$ with an excess of L, 2×10^{-4} or $5 \times 10^{-4} \text{ M}$, to ensure the complexation of the uranyl ion) with sodium perchlorate solutions in concentrations of 5×10^{-3} – $5 \times 10^{-2} \text{ M}$ (after mixing). For

(1) Moskovits, M.; Ozin, G. A. *Cryochemistry*; Wiley-Interscience: New York, 1976.

(2) McCaffrey, J. G.; Ozin, G. A. *J. Am. Chem. Soc.* **1982**, *104*, 7351.

(3) Liesegang, G.; Farrow, M.; Vazquez, F.; Purdie, N.; Eyring, E. *J. Am. Chem. Soc.* **1977**, *99*, 3240.

(4) Petrucci, S.; Adamic, R.; Eyring, E. *J. Phys. Chem.* **1986**, *90*, 1677.

(5) Chen, C.; Wallace, W.; Eyring, E.; Petrucci, S. *J. Phys. Chem.* **1984**, *88*, 2541.

(6) Chen, C.; Wallace, W.; Eyring, E.; Petrucci, S. *J. Phys. Chem.* **1984**, *88*, 5445.

(7) Maynard, K.; Irish, D.; Eyring, E.; Petrucci, S. *J. Phys. Chem.* **1984**, *88*, 729.

(8) Chen, C.; Petrucci, S. *J. Phys. Chem.* **1982**, *86*, 2601.

(9) Strasser, B.; Hallenga, K.; Popov, A. *J. Am. Chem. Soc.* **1985**, *107*, 789.

(10) Fux, P.; Lagrange, J.; Lagrange, P. *J. Am. Chem. Soc.* **1985**, *107*, 5927.

(11) Gosse, B.; Denat, A. *J. Electroanal. Chem. Interfacial Electrochem.* **1974**, *56*, 129.

(12) Kolthoff, I.; Harris, W. *J. Am. Chem. Soc.* **1945**, *67*, 1484.

(13) Lagrange, J.; Lagrange, P. *J. Chim. Phys.-Chim. Biol.* **1984**, *81*, 425.

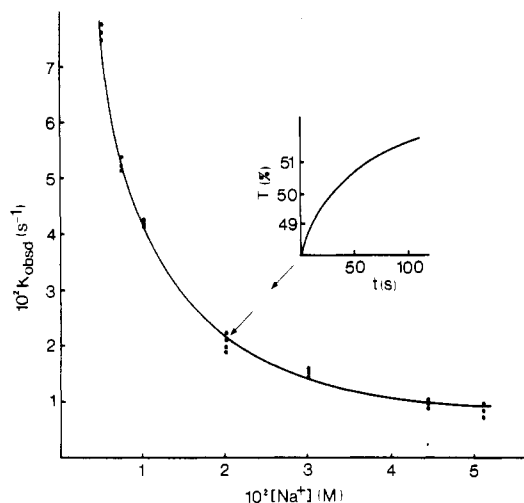


Figure 1. Pseudo-first-order observed rate constants for the reaction between the UO_2L^{2+} complex and Na^+ . The points are experimental data, and the curve corresponds to recalculated k_{obsd} values. The curve T (percent transmittance) = $f(t)$ gives an example of experimental data obtained with a solution where concentrations after mixing are as follows: $[\text{U(VI)}] = 1.375 \times 10^{-4} \text{ M}$; $[\text{L}] = 5.039 \times 10^{-4} \text{ M}$; $[\text{Na}^+] = 2.0 \times 10^{-2} \text{ M}$. $\lambda = 290 \text{ nm}$.

Na^+ concentrations lower than $5 \times 10^{-3} \text{ M}$ the variation of the spectrophotometric signal becomes too small to allow k_{obsd} measurements.

Results and Discussion

Thermodynamic results have shown that macrocyclic polyethers form stable complexes with the Na^+ ion and give a 1:1 complex¹² ($\log \beta = 5.6$) in PC solutions. We have previously observed that 18-crown-6 reacts with the uranyl ion to give a 1:1 complex^{12,13} ($\log \beta = 5.30$) in the same medium. In this complex, the uranyl ion is encapsulated in the macrocycle cavity (the "inclusive" complex $\text{UO}_2\text{L}^{2+}_{\text{incl}}$).

Under the experimental conditions chosen in this work, the uranyl solution contained, before reaction, the macrocyclic agent in a sufficient excess to form at least 96% of $\text{UO}_2\text{L}^{2+}_{\text{incl}}$. The variations in the concentration of the free ligand in excess did not have an effect on our kinetic data. The large excess of the Na^+ ion, in each kinetic experiment, ensures that the exchange reaction between UO_2^{2+} and Na^+ should take place quantitatively. The conditions were such that the reaction is pseudo first order and the reverse reaction in eq 1 can be neglected.

The plot of $\ln |A_t - A_\infty|$ vs time is linear for over 95% of the reaction (A_t and A_∞ are the absorbances of the system at reaction times t and ∞ , respectively). Each value of k_{obsd} , the pseudo-first-order rate constant, is the average of at least three determinations. k_{obsd} decreases with increasing Na^+ concentration (Figure 1) and may be written as a hyperbolic function:

$$k_{\text{obsd}} = \frac{A}{1 + B[\text{Na}^+]} \quad (2)$$

The A and B parameters were adjusted by least-squares analysis and will be explained by the proposed mechanism: $A = 0.41 \pm 0.02 \text{ s}^{-1}$ and $B = 890 \pm 30 \text{ dm}^3 \text{ mol}^{-1}$. Five preliminary remarks may be made with the object of postulating a consistent mechanism.

(1) Previous kinetic results have shown⁸ that the formation of the $\text{UO}_2\text{L}^{2+}_{\text{incl}}$ complex proceeds in three steps involving different intermediate species. In the first step two outer-sphere complexes between one solvated uranyl ion and one or two molecules of the entering ligand (18-crown-6) lead to an "external" complex where the coordination center is outside the macrocycle cavity. An "exclusive" complex, where the uranyl ion is partially inside the macrocycle cavity, is formed from the "external" complex by

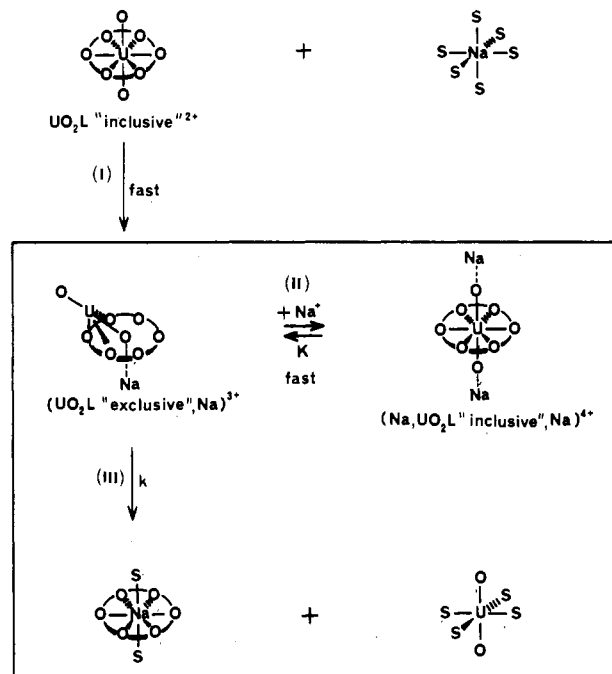
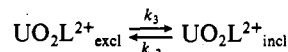


Figure 2. Mechanism of the reaction between the $\text{UO}_2\text{L}^{2+}_{\text{incl}}$ complex and the Na^+ ion. The numbers of solvent molecules in the inner solvation spheres of the different compounds are not known. Only some solvent molecules are drawn on the noncomplexed coordination centers Na^+ and UO_2^{2+} .

rotation of the uranyl group with resulting metal and ligand cavity desolvations. The third step is the rearrangement reaction



with

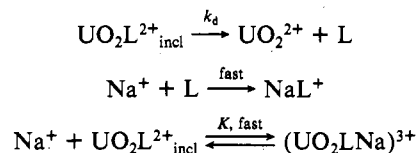
$$k_3 + k_{-3} = 0.022 \text{ s}^{-1}$$

(2) In recent studies, Popov et al.^{14,15} have shown that the complexation of K^+ or Na^+ with 18-crown-6 proceeds via a bimolecular exchange step with the formation of symmetrical dicationic species in the transition state. Analogous dicationic species were found by Detellier et al.¹⁶ in the exchange kinetics of the sodium cation with the larger ligand dibenzo-24-crown-8.

(3) Generally, the exchange of a multidentate ligand between two metal ions proceeds through a binuclear intermediate¹⁷⁻¹⁹ in which the entering and leaving metal ions are bonded to the ligand. The dissociation of this intermediate is often the rate-determining step of the overall process.

(4) The rate of complexation of Na^+ by 18-crown-6 is too fast to be measured by the stopped-flow technique.

(5) The inhibition effect of Na^+ in eq 2 must be due to the presence of two species in equilibrium: one is a productive intermediate, the other, which has a larger stoichiometry in Na , is a "dead end". Consequently, one may propose



The calculated rate law and eq 2 give $k_d = 0.41 \text{ s}^{-1}$ and $K = 890 \text{ M}^{-1}$.

(12) Fux, P.; Lagrange, J.; Lagrange, P. *Anal. Chem.* **1984**, *56*, 160.

(13) Brighli, M.; Fux, P.; Lagrange, J.; Lagrange, P. *Inorg. Chem.* **1985**, *24*, 80.

(14) Schmidt, E.; Popov, A. *J. Am. Chem. Soc.* **1983**, *105*, 1873.

(15) Strasser, B.; Hallenga, K.; Popov, A. *J. Am. Chem. Soc.* **1985**, *107*, 789.

(16) Delville, A.; Stöver, H.; Detellier, C. *J. Am. Chem. Soc.* **1985**, *107*, 4172.

(17) Bydalek, T.; Margerum, D. *Inorg. Chem.* **1963**, *2*, 678.

(18) Brücher, E.; Laurency, G. *Inorg. Chem.* **1983**, *22*, 338.

(19) Mentasti, E. *J. Chem. Soc., Dalton Trans.* **1984**, 903.

In this proposed mechanism the $\text{UO}_2\text{L}^{2+}_{\text{incl}}$ decomplexation must proceed via the $\text{UO}_2\text{L}^{2+}_{\text{excl}}$ intermediate. The first preliminary remark above shows that k_d must be less than 0.022 s^{-1} . As this mechanism cannot explain the kinetic results, a mechanism is given (Figure 2) and discussed as follows.

In the first step (step I), which appears to be instantaneous when the stopped-flow technique is used, a direct interaction of the Na^+ ion with the $\text{UO}_2\text{L}^{2+}_{\text{incl}}$ complex gives rise to the $(\text{UO}_2\text{L}_{\text{excl}}, \text{Na})^{3+}$ intermediate species. This intermediate is probably an outer-sphere complex where the coordinating center UO_2^{2+} is partially enclosed in the ligand cavity and where the Na^+ ion is incompletely desolvated. The $(\text{UO}_2\text{L}_{\text{excl}}, \text{Na})^{3+}$ complex is instantaneously in equilibrium (step II) with a second outer-sphere complex $(\text{Na}, \text{UO}_2\text{L}_{\text{incl}}, \text{Na})^{4+}$. In the UO_2^{2+} ion, the effective electrical charge on the U atom is considerably higher than the total charge (+2) of the entity and the two oxygen atoms carry a net negative charge.²⁰ Then, two solvated Na^+ ions may enter into the second solvation shell of the $\text{UO}_2\text{L}^{2+}_{\text{incl}}$ complex and interact with the two oxygens of the uranyl ion. These fast steps I and II are followed by the total rotation of the uranyl group on the outside of the ligand cavity and by the uranyl-18-crown-6 bond rupture in the $(\text{UO}_2\text{L}_{\text{excl}}, \text{Na})^{3+}$ complex (step III). This last step is rate-determining and leads to the final product when the Na^+ ion has been completely and instantaneously buried in the host cavity. The $(\text{Na}, \text{UO}_2\text{L}_{\text{incl}}, \text{Na})^{4+}$ complex, in which the loss of the uranyl ion is hindered by the two Na^+ ions, would not give a rearrangement reaction leading to the NaL^+ complex. The mathematical treatment of this mechanism leads to the following equations, which agree with the experimental data:

$$-\frac{d[\text{UO}_2\text{L}]_{\text{T}}}{dt} = k_{\text{obsd}}[\text{UO}_2\text{L}]_{\text{T}} = k[(\text{UO}_2\text{L}_{\text{excl}}, \text{Na})^{3+}]$$

$$[\text{UO}_2\text{L}]_{\text{T}} = [(\text{UO}_2\text{L}_{\text{excl}}, \text{Na})^{3+}] + [(\text{Na}, \text{UO}_2\text{L}_{\text{incl}}, \text{Na})^{4+}]$$

$$k_{\text{obsd}} = \frac{k}{1 + K[\text{Na}^+]}$$

$$k = 0.41 \pm 0.02 \text{ s}^{-1}; K = 890 \pm 30 \text{ dm}^3 \text{ mol}^{-1}$$

Only the third step is experimentally observed.

Some experiments done with Na^+ concentrations of 10^{-4} – 10^{-3} M do not allow us to observe steps I and II, but the existence of these preliminary fast steps is supported by the measurement and the calculation of the absorbances corresponding to time zero for each kinetic experiment. The measured values are obtained by extrapolation of the experimental kinetic curves and the calculated ones by addition of the absorbances of each reactant after mixing and fast complexation of the excess free ligand. Small differences between these two values were observed, indicating fast preliminary steps.

Registry No. UO_2L^{2+} , 56508-54-4; Na^+ , 17341-25-2.

(20) Ahrland, S.; Liljenzin, J.; Rydberg, J. *Comprehensive Inorganic Chemistry*; Pergamon: New York, 1973; Vol. 5.

Contribution from the Department of Chemistry,
University of Idaho, Moscow, Idaho 83843

Carbonyl Difluoride: A Fluorinating Reagent for Inorganic Oxides

S. P. Mallela, O. D. Gupta, and Jean'ne M. Shreeve*

Received May 19, 1987

Carbonyl difluoride (COF_2) has been demonstrated to be a highly versatile reagent for introducing fluorine into a variety of different molecules either by oxidative addition of fluorine to the central atom or by the displacement of hydrogen by fluorine from

Table I. Experimental Details of Fluorination of Inorganic Oxides with COF_2

group	reactant (2–3 mmol)	temp, °C	time, h	products: CO_2^+	yield, ^a %
5	V_2O_5	210	34	VOF_3	~100
	Nb_2O_5	200	36	NbF_5	~100
	Ta_2O_5	210	46	TaF_5	~100
6	CrO_3^b	185	12	CrO_2F_2	~100
	MoO_3	190	31	MoOF_4	~100
	WO_3	180	48	WOF_4	~100
	MnO_2	170	60	NR ^c	
8	OsO_4	90 or 150	22 (AHF) ^f	NR	
9	Co_2O_3	200	168	NR	
10	NiO	180	168	NR	
12	HgO (red)	160	36	NR	
	HgO (yellow)	200	36	NR	
13	B_2O_3	150	36	BF_3	~92
14	SiO_2	160	36	SiF_4	~100
	GeO_2	100	24	GeF_4	~84
	SnO_2^d	220	70	SnF_4	~100
	SnO_2	210	80	SnF_4	~50
	PbO_2	200	24	NR	
15	P_4O_{10}	180	24	$\text{PF}_5, \text{OPF}_3$	~65
16	SO_2^d	200	86	NR	
	SeO_2	200	50	SeOF_2	~100
	TeO_2	160	56	TeF_4	~100
	I_2O_5	160	36	IF_5	~60
17	UO_3^e	180	45	UO_2F_2	~100
	UO_3^d	210	27	UO_2F_2	~100

^aBased on CO_2 formed. ^bReference 4. ^cNo reaction. ^dIn presence of small amount of CsF. ^eReference 3. ^fAnhydrous hydrogen fluoride.

P–H, N–H, or C–H bonds.¹ We now report the results obtained when COF_2 is reacted with main-group and transition-metal oxides to provide a new simple route to useful fluorinated compounds.

The conversion of inorganic oxides to fluorides can be accomplished in a large number of ways by using vigorous fluorinating reagents such as elemental fluorine or bromine trifluoride or with milder reagents such as anhydrous hydrogen fluoride or sulfur tetrafluoride. However, these fluorination methods often suffer from certain drawbacks, such as forming byproducts that are difficult to separate from the inorganic fluoride product or that are difficult to destroy. However, COF_2 is easily synthesized² and it reacts readily under mild conditions to form volatile CO_2 as the only byproduct. Carbon dioxide is easily removed from the reaction vessel and absorbed in alkali. Following the formation of the CO_2 via infrared spectral examination provides a good method for monitoring the progress of the reaction.

Experimental Section

General Procedure. A known amount (~2–3 mmol) of the anhydrous, powdered metal oxide or non-metal oxide was loaded into a 75-mL stainless steel or Monel Hoke cylinder fitted with a stainless steel or Monel Whitey valve. A slight excess over the stoichiometric amount of COF_2 required was condensed into the cylinder at -196°C by using standard vacuum-line techniques (except $\text{SnO}_2:\text{COF}_2 = 1:4$ and $\text{Nb}_2\text{O}_5:\text{COF}_2 = 1:8$). The neat reaction mixture was then heated in an oven, with occasional shaking. After the reaction had finished, the presence of COF_2 and CO_2 was checked by examining their infrared spectra. All of the fluoride products were confirmed by comparison of infrared and ^{19}F NMR spectral data with literature values. *Caution!* Carbonyl difluoride is a highly toxic compound and should be handled accordingly.

Results and Discussion

Representative inorganic oxides were selected to cover most of the periodic table from group 5 to group 17. Oxides such as UO_3 were of particular interest in our static system since the fluorination of the former in a CO_2 flow system at 750°C resulted in 97.6% conversion to UF_6 .³ We obtained essentially quantitative

- (1) Gupta, O. D.; Shreeve, J. M. *J. Chem. Soc., Chem. Commun.* **1984**, 416 and references therein. Williamson, S. M.; Gupta, O. D.; Shreeve, J. M. *Inorg. Synth.* **1986**, *24*, 62.
- (2) PCR Research Chemicals, Inc., P.O. Box 1778, Gainesville, FL 32602. Fawcett, F. S.; Tullock, C. W.; Coffman, D. D. *J. Am. Chem. Soc.* **1962**, *84*, 4275.
- (3) Neto, J. A. P.; Costa, E. C.; Sareyed-Dim, N. A. Braz. Pedido PI 8 000 195, Nov 4, 1980; *Chem. Abstr.* **1981**, *94*, 159099b.